AFRL-SN-WP-TR-2006-1169

RADIATION AND SCATTERING COMPACT ANTENNA LABORATORY

Joshua Radcliffe

RF/EO Subsystems Branch (AFRL/SNDR)
Aerospace Components Division
Sensors Directorate
Air Force Research Laboratory, Air Force Materiel Command
Wright-Patterson Air Force Base, OH 45433-7320

SEPTEMBER 2006

Interim Report for 01 May 2004 – 01 May 2006

SENSORS DIRECTORATE
AIR FORCE RESEARCH LABORATORY
AIR FORCE MATERIEL COMMAND
WRIGHT-PATTERSON AIR FORCE BASE, OH 45433-7320

NOTICE AND SIGNATURE PAGE

Using Government drawings, specifications, or other data included in this document for any purpose other than Government procurement does not in any way obligate the U.S. Government. The fact that the Government formulated or supplied the drawings, specifications, or other data does not license the holder or any other person or corporation; or convey any rights or permission to manufacture, use, or sell any patented invention that may relate to them.

This report was cleared for public release by the Air Force Research Laboratory Wright Site (AFRL/WS) Public Affairs Office and is available to the general public, including foreign nationals. Copies may be obtained from the Defense Technical Information Center (DTIC) (http://www.dtic.mil).

AFRL-SN-WP-TR-2006-1169 HAS BEEN REVIEWED AND IS APPROVED FOR PUBLICATION IN ACCORDANCE WITH ASSIGNED DISTRIBUTION STATEMENT.

*//Signature//

JOSHUA RADCLIFFE, Project Engineer
RF/EO Subsystems Branch
Aerospace Components Division

//Signature//

GEORGE SIMPSON, Chief
RF/EO Subsystems Branch
Aerospace Components Division

//Signature//

TODD A. KASTLE, Chief
Aerospace Components Division
Sensors Directorate

This report is published in the interest of scientific and technical information exchange and its publication does not constitute the Government's approval or disapproval of its ideas or findings.

*Disseminated copies will show "//signature//" stamped or typed above the signature blocks.

REPORT DOCUMENTATION PAGE

Form Approved
OMB No. 0704-0188

1. REPORT DATE *(DD-MM-YY)*	2. REPORT TYPE	3. DATES COVERED *(From - To)*
September 2006	Interim	05/01/2004 – 05/01/2006

4. TITLE AND SUBTITLE
RADIATION AND SCATTERING COMPACT ANTENNA LABORATORY

5a. CONTRACT NUMBER
In-house

5b. GRANT NUMBER

5c. PROGRAM ELEMENT NUMBER
62204F

6. AUTHOR(S)
Joshua Radcliffe

5d. PROJECT NUMBER
7622

5e. TASK NUMBER
11

5f. WORK UNIT NUMBER
0D

7. PERFORMING ORGANIZATION NAME(S) AND ADDRESS(ES)

RF/EO Subsystems Branch (AFRL/SNDR)
Aerospace Components Division
Sensors Directorate
Air Force Research Laboratory, Air Force Materiel Command
Wright-Patterson Air Force Base, OH 45433-7320

8. PERFORMING ORGANIZATION REPORT NUMBER
AFRL-SN-WP-TR-2006-1169

9. SPONSORING/MONITORING AGENCY NAME(S) AND ADDRESS(ES)

Sensors Directorate
Air Force Research Laboratory
Air Force Materiel Command
Wright-Patterson AFB, OH 45433-7320

10. SPONSORING/MONITORING AGENCY ACRONYM(S)
AFRL-SN-WP

11. SPONSORING/MONITORING AGENCY REPORT NUMBER(S)
AFRL-SN-WP-TR-2006-1169

12. DISTRIBUTION/AVAILABILITY STATEMENT
Approved for public release; distribution is unlimited.

13. SUPPLEMENTARY NOTES
Report contains color. PAO Case Number: AFRL/WS-06-2424, 12 Oct 2006.

14. ABSTRACT
In-house applied RF aperture development in the RASCAL laboratory. This interim report contains research centered on leaky wave antenna technology and wideband spiral antenna interferometry. Novel, thin profile, wideband apertures (leaky wave phenomena) have a bright future amongst small vehicle installation. Robust modeling, fabrication, and in-house measurement have led to unique breakthroughs in bandwidth, high efficiency, and end termination schemes. Wideband spiral antenna interferometry has been a new area of direction finding which brings wideband performance to the accuracy of interferometric systems. The validation of this system performance was successfully accomplished via in-house design and measurements.

15. SUBJECT TERMS
RF apertures, wideband, direction finding, thin profile

16. SECURITY CLASSIFICATION OF:			17. LIMITATION OF ABSTRACT:	18. NUMBER OF PAGES	19a. NAME OF RESPONSIBLE PERSON (Monitor)
a. REPORT	b. ABSTRACT	c. THIS PAGE			Joshua Radcliffe
Unclassified	Unclassified	Unclassified	SAR	24	19b. TELEPHONE NUMBER *(Include Area Code)* N/A

Standard Form 298 (Rev. 8-98)
Prescribed by ANSI Std. Z39-18

Radiation and Scattering Compact Antenna Laboratory
RASCAL

Novel Wideband Conformal Apertures

Purpose and Payoff

It is well known that a microstrip transmission line can radiate if it is excited in its first higher order mode (with the fundamental or dominant mode suppressed). A new microstrip configuration is proposed that supports the first higher order mode while suppressing the fundamental mode. Hence, it is theoretically feasible to realize a traveling wave antenna using microstrip transmission lines if properly developed. This aperture will in principle have wide bandwidth, an "end-fire" radiation pattern, high efficiency, and be ultra thin (much less than one quarter of a wavelength). A new configuration of this approach is being researched in RASCAL to exploit this microstrip technology for lightweight, low cost, facile fabrication of wideband apertures.

Leaky Wave Phenomena Research

A leaky wave antenna is a special form of traveling wave antenna characterized by a wave propagating interior to a guiding structure rather than exterior as in the case of a Beverage antenna. As seen in Figure 1, the dominant mode of a standard microstrip line does not radiate since the guided wave underneath the microstrip is coherent. However, when the dominant mode is suppressed, the first higher order mode undergoes a phase reversal of the electric field along a centered vertical axis, as shown in figure 2, and radiation of the first higher order mode occurs.

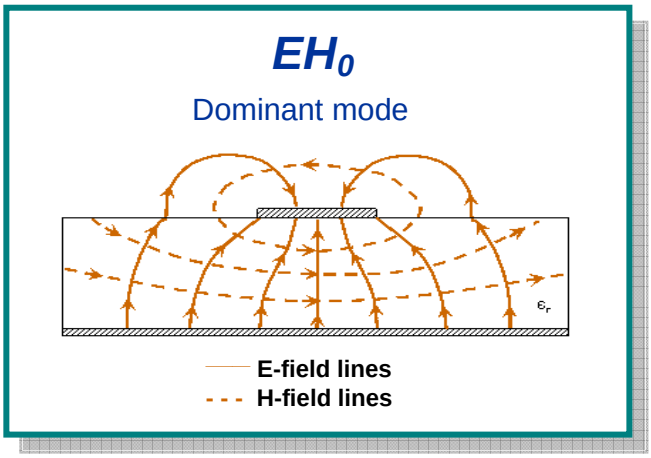

Figure 1: The electric field distribution of the dominant mode (does not radiate).

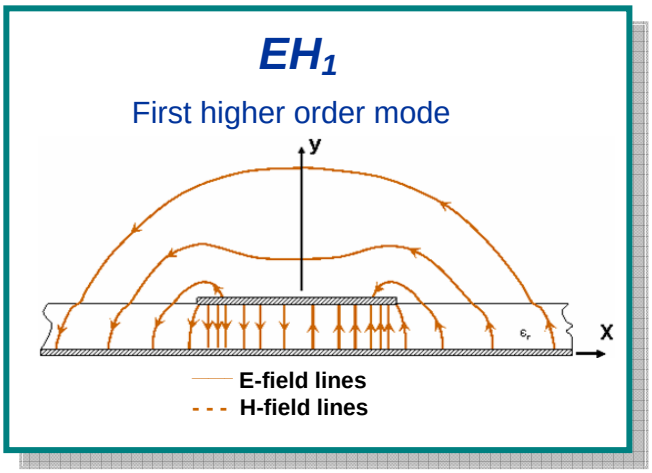

Figure 2: The electric field distribution of the EH_1 mode.

This guided-wave energy sets up a leaky wave exterior to the guiding structure and "leaks or sheds" power away from the guiding structure in a controlled way as the mode propagates from the feed to the termination. In doing so, radiation occurs with a peak that squints in the direction of propagation, as is the case with a Beverage antenna; however, this configuration is amenable to conformal installation. Menzel proposed an interesting example of a leaky wave antenna. His design [1], shown in Figure 3, is a wide microstrip line with several rectangular slots close to the feed end of the antenna along the centerline of the microstrip. These slots create a null electric field, or a virtual ground, at the center of the microstrip causing this mode to short to ground (see Figure 1 for the field distribution of this mode). Doing so allows the first higher order mode to propagate along the length of the microstrip since that mode already has an electric field null along the centerline (see Figure 2). Figure 4 illustrates Menzel's antenna design as fabricated in AFRL/SNRR's RASCAL Laboratory.

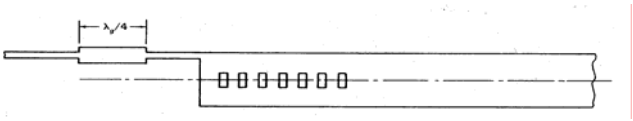
Figure 3: Menzel's Leaky Wave Antenna design.

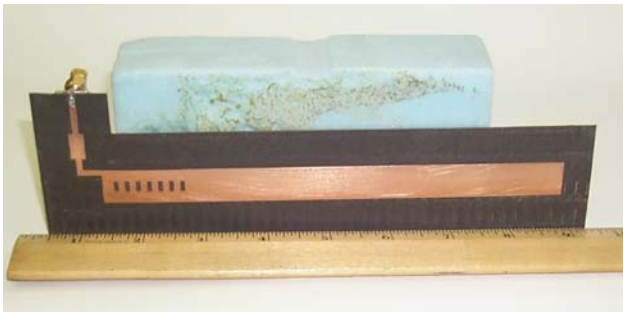
Figure 4: Menzel's Antenna fabricated and tested in RASCAL.

A new configuration of this type of leaky wave microstrip antenna design is proposed in Figure 5. To prevent the propagation of the fundamental mode, closely spaced metal posts may be placed longitudinally along the centerline of the microstrip. This physical

null in the electric field suggests half of the antenna width can be discarded without impacting the suppression of the fundamental mode. This new configuration is shown in Figure 5. Since the footprint of the antenna is now smaller, an array of such elements can be packed closer together with less mutual coupling between elements. Figure 6 shows this new "half-width" design as fabricated and tested in RASCAL [2].

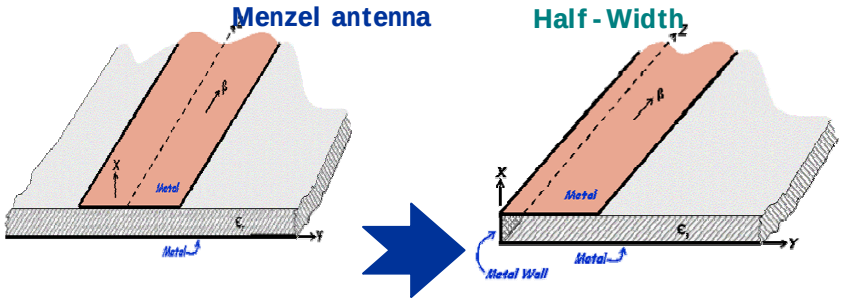

Figure 5: Menzel's design compared to the new "half-width" design.

Figure 6: New "half-width" design fabricated and tested in RASCAL.

Dr. Thiele has also implemented this "half-width" design into alternate arrangements searching for a design of maximum performance. Figure 7 shows a curved half-width arrangement, while figure 8 shows stepped and sloped half-width arrangements. These alternate designs have just begun to be studied in detail and initial measurements have been taken in the RASCAL compact range.

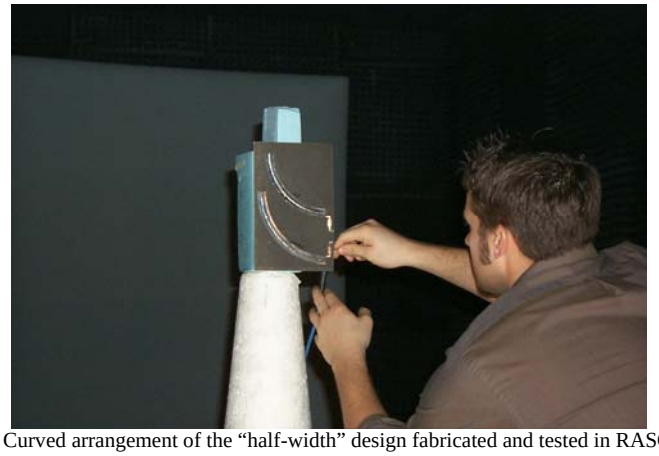

Figure 7: Curved arrangement of the "half-width" design fabricated and tested in RASCAL.

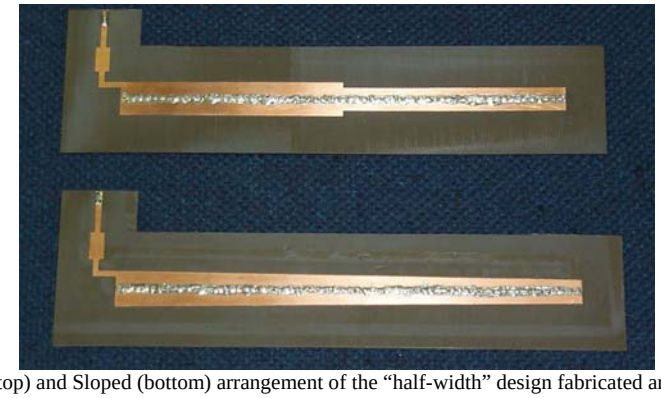

Figure 8: Stepped (top) and Sloped (bottom) arrangement of the "half-width" design fabricated and tested in RASCAL.

Leaky Wave Measurements

Both Menzel and "half-width" antenna designs were fabricated on Rogers 5870 duroid substrate made of PTFE glass fiber with a dielectric constant of $\varepsilon_r = 2.33$ and a thickness of .787 mm. The length of each antenna is 190 mm beginning where the width opens up to maximum width and ending at the antenna terminus. The Menzel design width is 15 mm while the width of the half-width aperture is, obviously, 7.5 mm. Figure 9 shows pattern measurements made in the RASCAL compact range. These results indicate that the configuration in Figure 6 produces a similar radiation pattern as the Menzel design (see Figure 4) with the reduced aperture footprint. Figure 9 illustrates a comparison of the measured far-field patterns at 6.7 GHz.

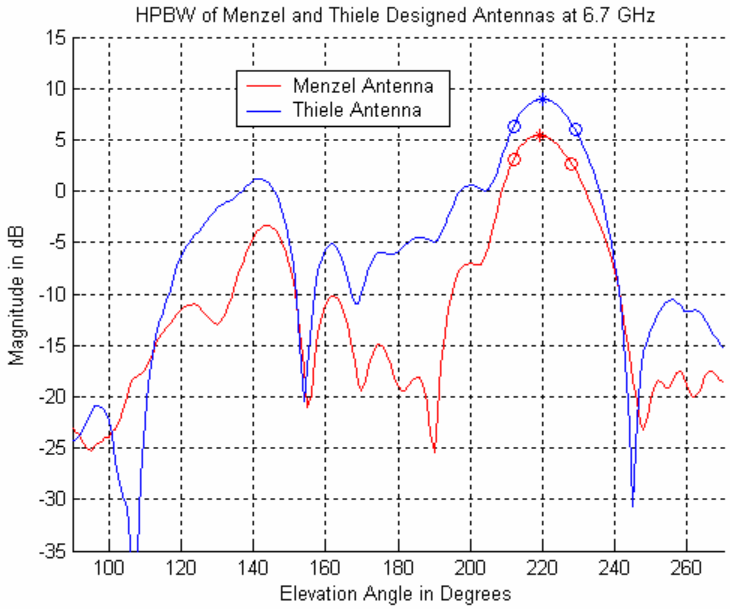

Figure 9: Menzel vs. Thiele for 6.7 GHz at the antenna orientation of figure 6.

Many measurements comparing these two designs have been taken at a band of frequencies from 6-8 GHz. As one can plainly see from Figure 9, there exists an

extremely large reflected beam on the left side of the plot. This exists due to the antenna not being fully matched and therefore all the energy is not radiated in one single direction. Future research endeavors to completely match the antenna thereby eliminating the reflected lobe and allowing the maximum radiation in a near endfire direction. Other future research for this task includes maximizing bandwidth of the "half-width" design. Many avenues exist for us to accomplish this goal, including: spiral half-width configuration, different dielectric configurations, and determining the most effective means of terminating the antenna.

FE-BI Analysis with a Resistive Sheet Termination

Efforts have begun to determine the best means to match and terminate this leaky wave half-width design to achieve the best performance. Dr. Leo Kempel, an IPA from Michigan State University, has been studying the effects of a simple R-Card termination on a half-width antenna using finite element—boundary integral (FE-BI) analysis.

The FE-BI method has been extensively reported upon in the literature and is extensively discussed in at least three popular text books on finite element methods for high frequency electromagnetics.

The half-width antenna utilizes a physical electric conducting wall to suppress the fundamental EH_0 mode. This is accomplished in the finite element model with periodic 1Ω resistors (in the actual antenna constructed in RASCAL at AFRL/SNRR, the wall is formed with conducting pins). The feed is a probe feed placed approximately half-way along the width of the half-width antenna and slightly inset. According to (1), the leaky-wave region of the antennas is given by $6.55\,\text{GHz} \le f \le 8.67\,\text{GHz}$. Below this range of frequency, the EH_1 mode is in cut-off while above that range, the bound mode is dominant. In [3], the data generated from both the FDTD and transverse resonance models indicate that the attenuation of the propagating wave is quite small in the leaky-wave band and hence, a relatively short antenna (as is the one in this work) will have a significant backward traveling leaky-wave.

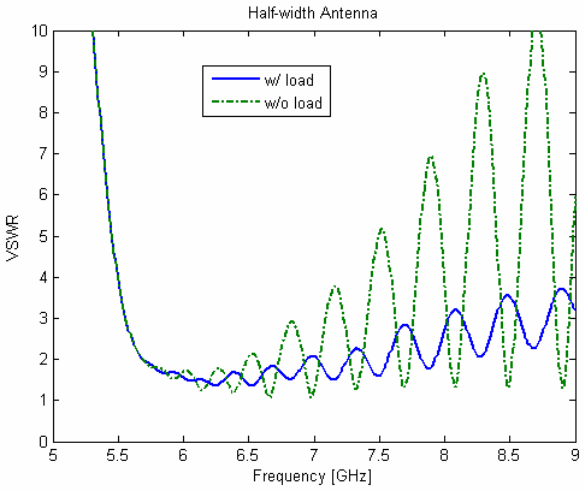

Figure 10: Comparison of the VSWR for a loaded and unloaded half-width antenna.

This FE-BI analysis considers the impact of placing a tapered resistive sheet condition at the end of the microstrip antenna. The purpose of which it to reduce the level of a backward traveling wave and hence realize as close as possible the forward traveling wave results used to design such antennas. Note that this termination is physically realizable in comparison with the purely numerical termination. The choice of the taper is based upon an understanding of the leaky traveling wave. It is analogous to the traveling wave excited by TE_z incident field impinging on a PEC half-plane. Studies in the past have suggested the use of a gradual resistivity taper to a moderate end resistivity is a good means of softening the diffraction from such a half-plane.

Hence, it is assumed that such a taper would also work well in reducing the reflection from a truncated leaky-wave microstrip line. For this work, a quadratic taper from $1\Omega/\text{sq.}$ to $50\Omega/\text{sq.}$ over a 3 cm length is used. This length was chosen to keep the over-all length of the antenna relatively small.

The VSWR (assuming a 50Ω feedline) is shown in Figure 10 comparing the VSWR of the unloaded and loaded antenna. As can be seen, the load has a significant effect on the VSWR for the leaky-wave region resulting in much less variation in VSWR w.r.t. frequency.

A comparison of the radiation pattern for the loaded and unloaded half-width antennas at 6.7 GHz is shown in Figure 11. The unloaded results are comparable to those presented in [3] in terms of the location of the peak radiation and in the front-to-back ratio. As can be seen, the front-to-back ratio is dramatically improved (on the order of 10 dB) through the use of the resistive sheet termination.

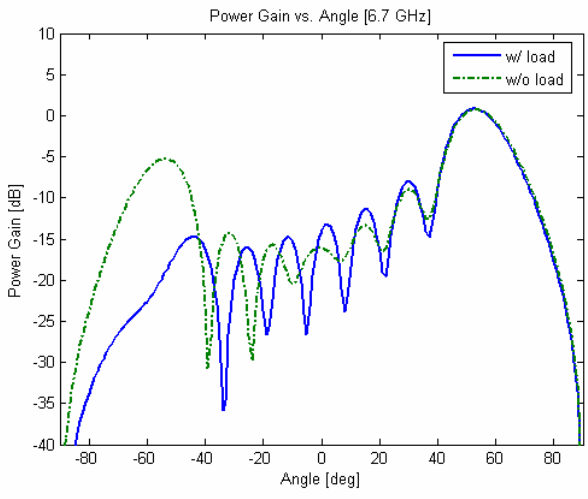

Figure 11: Comparison of power gain patters for the loaded and unloaded half-width antennas at 6.7 GHz.

Both the impedance results and the increase in front-to-back ratio are explained by investigating the normal electric field component (E_z) as a function of position in the computational domain. Figure 6 illustrates the electric fields, at 6.7 GHz, for the unloaded case.

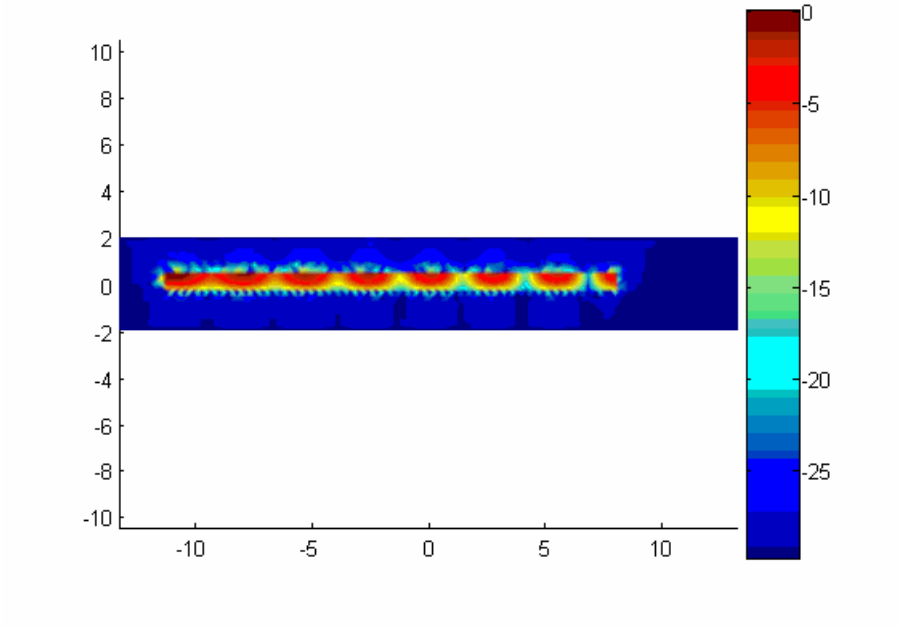

Figure 12: Normal electric fields for the unloaded half-width antenna at 6.7 GHz.

As can be seen, a significant standing wave is present due to the interaction between forward and backward traveling leaky-waves. For the loaded case, the backward wave is significantly reduced (see Figure 11) and hence the standing wave is reduced. This is shown in Figure 13.

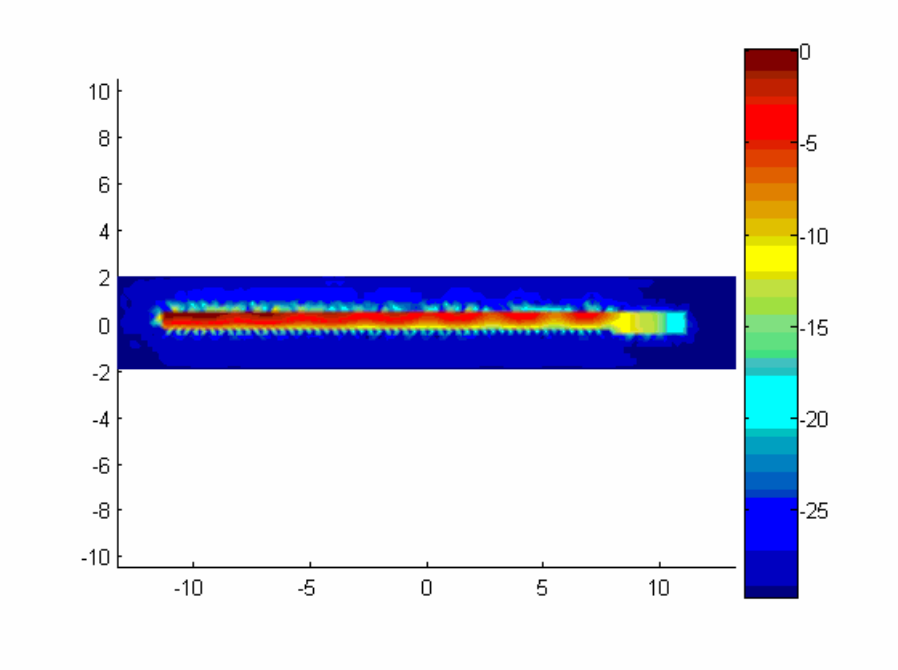

Figure 13: Normal electric fields for the loaded half-width antenna at 6.7 GHz.

As a final example of the impact of the edge treatment, consider the same antenna operated at 8 GHz (shown in Figure 14). In this case, the gain is dramatically lower than the case at 6.7 GHz. Note that if no edge treatment is applied, the front-to-back ratio is nearly 0 dB!

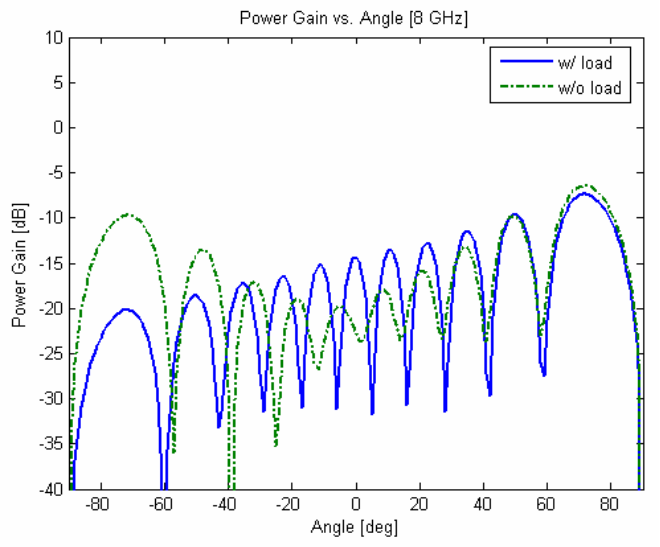

Figure 14: Comparison of loaded and unloaded half-width antennas' power gain patterns at 8 GHz.

FDTD Simulations

1Lt. Greg Zelinski performed many in depth finite difference time domain (FDTD) simulations in RASCAL [3] as part of his masters degree thesis at the Air Force Institute of Technology (AFIT).

The antenna was excited by giving the E_y component in one or more cells a certain value. This source value was a sinusoid with a cubic ramp over the first three periods. The half-width antenna in Figure 5 was simulated using Matlab over 5.9 - 8.2 GHz, which is the bandwidth predicted by transverse resonance. The 3-D FDTD simulation was patterned after code written by K. Willis and S. Hagness of U. of Wisconsin Computational Electromagnetics Laboratory that used Uniaxial Perfectly Matched Layers (UPML). The ground plate and all conductors were modeled as PEC by setting the tangential electric field components to zero for the appropriate cells. The PEC structure was continued into the UPML in both ***x*** directions.

Computing resources were a limiting factor. The antenna is very thin (< 1 mm) and quite long (up to 1200 mm). Since nearly cubic cells improve FDTD accuracy, this shape creates the need for a huge number of cells. Several tests were run to determine the fewest number of cells needed to accurately model the antenna. The transverse resonance approximation was used as a yard stick to judge the FDTD simulations. The thickness of the UPML layer was found to be frequency dependent. Above 6.7 GHz, only 4 UPML cells proved adequate. Below 6.0 GHz, 16 cells were required. The transition between these points was not linear. The free space region above the antenna was reduced to just 2 cells thick with no noticeable degradation to the results. Likewise, only 2 cells of open substrate on either side of the conducting strip were needed. The tradeoffs between cell size and error were explored. As long as the cross-section dimensions were square, the longitudinal dimension could be five times as long as the cross section size with less than 1% error. The thickness of the substrate was reduced to 5 cells with no measurable effect. The number of cells in the longitudinal direction needed to extract at least two periods of the traveling wave was frequency dependent. The antenna at 5.9 GHz was required to be more than four times longer than the 8.2 GHz antenna. The outcome of these tests was the reduction of the number of cells required to 170,000 at 8.2 GHz and 2,250,000 at 5.9 GHz. This nearly 10-fold decrease in computations and 20-fold decrease in memory allowed all trials above 6.1 GHz to be run on a 3 GHz PC with 1 GB of RAM. The 5.9 - 6.1 GHz trials were run on a 2.5 GHz Mac G5 with 2.5 GB of RAM.

α and β were determined by matching a known $e^{-j\gamma z}$ curve to the E_y field amplitude of the same cross section cell as the source, along the length of the antenna. β was found from a least squares fit of the zero crossings and α was found from a least squares fit of the peak values. As seen in Figure 15, a radiation pattern can be estimated using $\gamma = \beta - j\alpha$ results in $I = I_0 e^{-j\gamma z}$ for a line source.

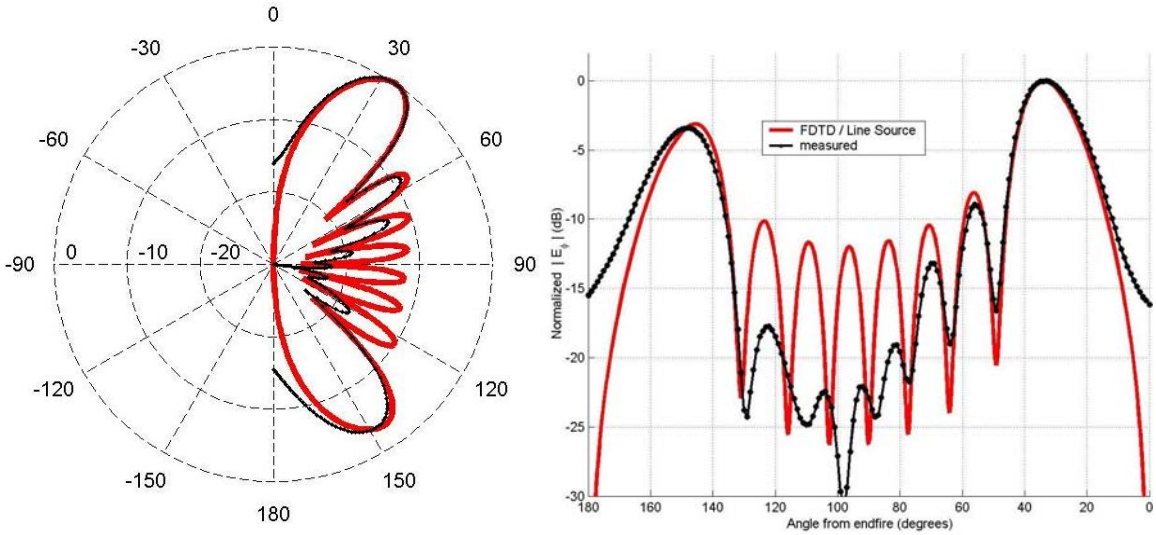

Figure 15: The H-plane radiation pattern of the half width antenna at 7.2 GHz from experimental measurements [2] and the line source approximation using FDTD results.

Leaky Wave Modeling & Simulation

Mr. John Reynolds, an SNRR co-op, has done electromagnetic modeling on both the Menzel and "half-width" antenna designs in CST Microwave Studio. The results from these simulations reiterate the measurements performed in RASCAL. The pattern shapes are congruent, but there is still minimal differences in the gain levels between the simulations and the measurements in RASCAL. Future work includes investigating these results in depth and understanding the idiosyncrasies of these gain differences. Figures 16-19 show the comparison between the modeling results and the measurements results from RASCAL.

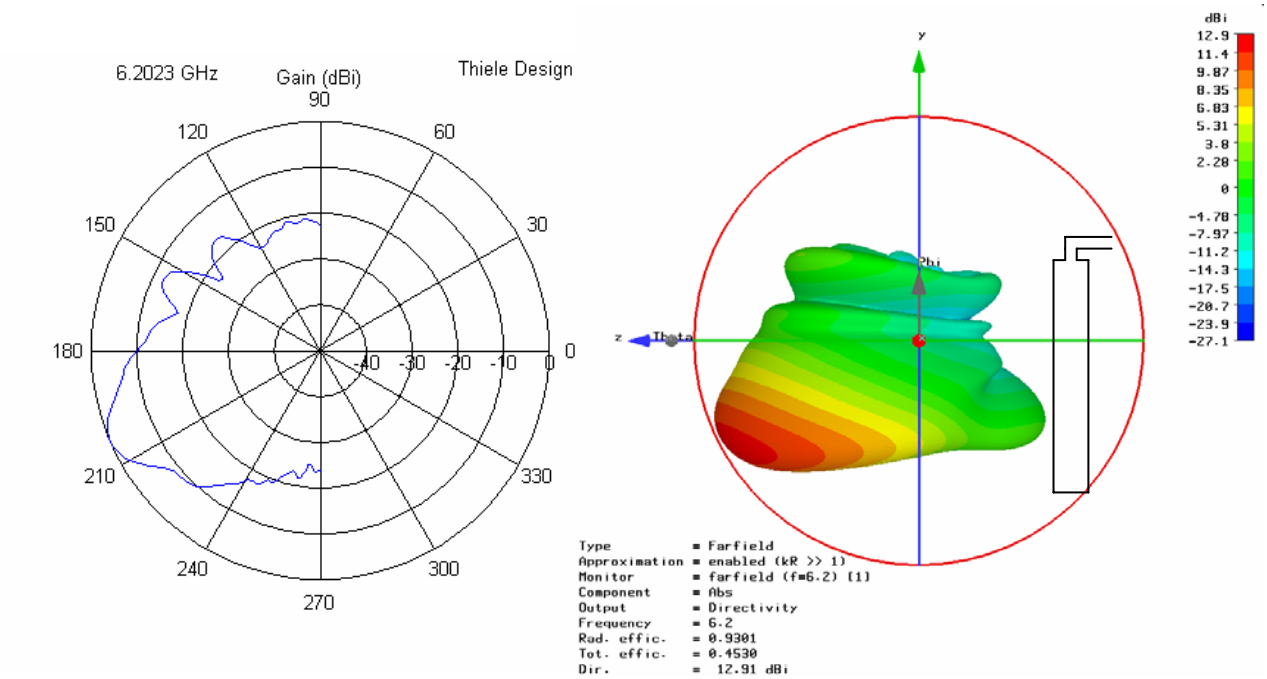

Figure 16: Measured (left) and Theoretical (right) comparison for 6.2 GHz.

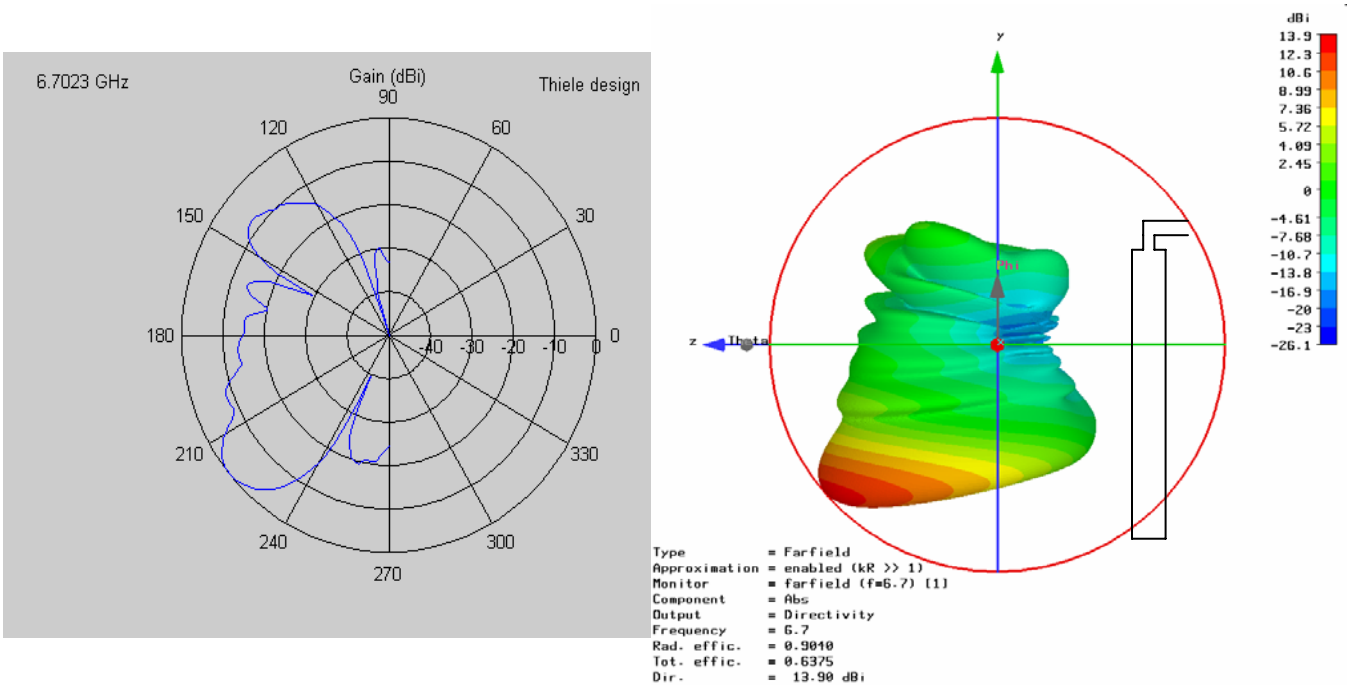

Figure 17: Measured (left) and Theoretical (right) comparison for 6.7 GHz.

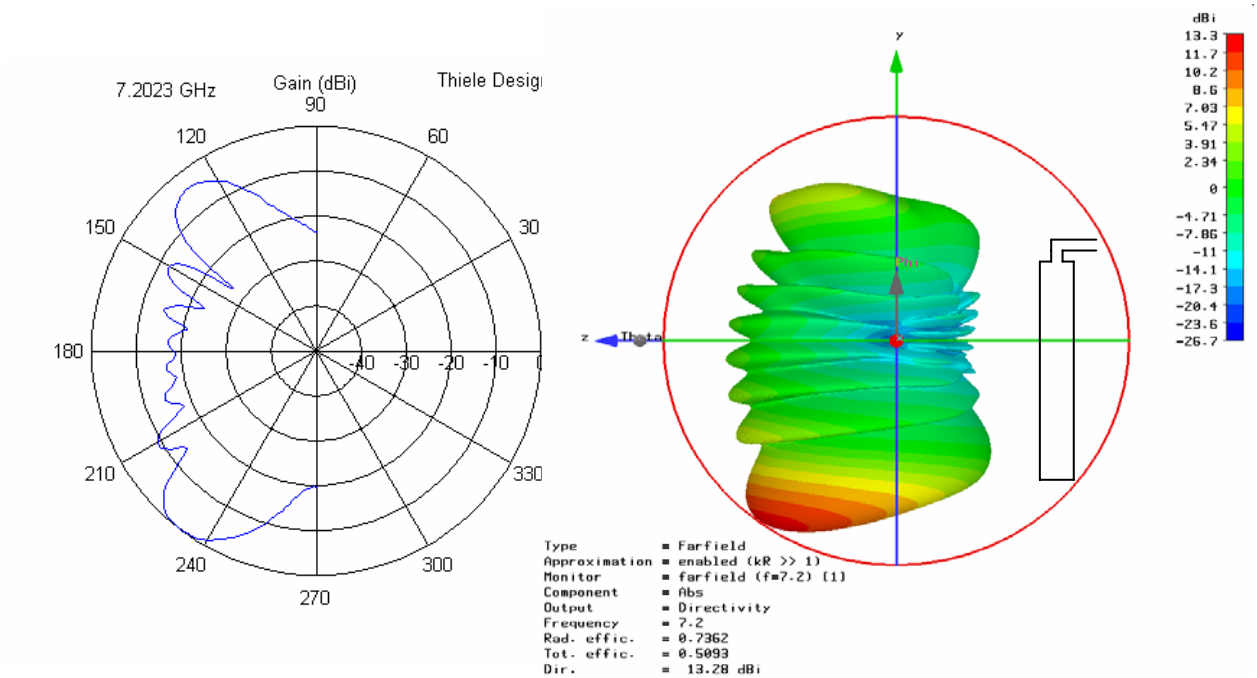

Figure 18: Measured (left) and Theoretical (right) comparison for 7.2 GHz.

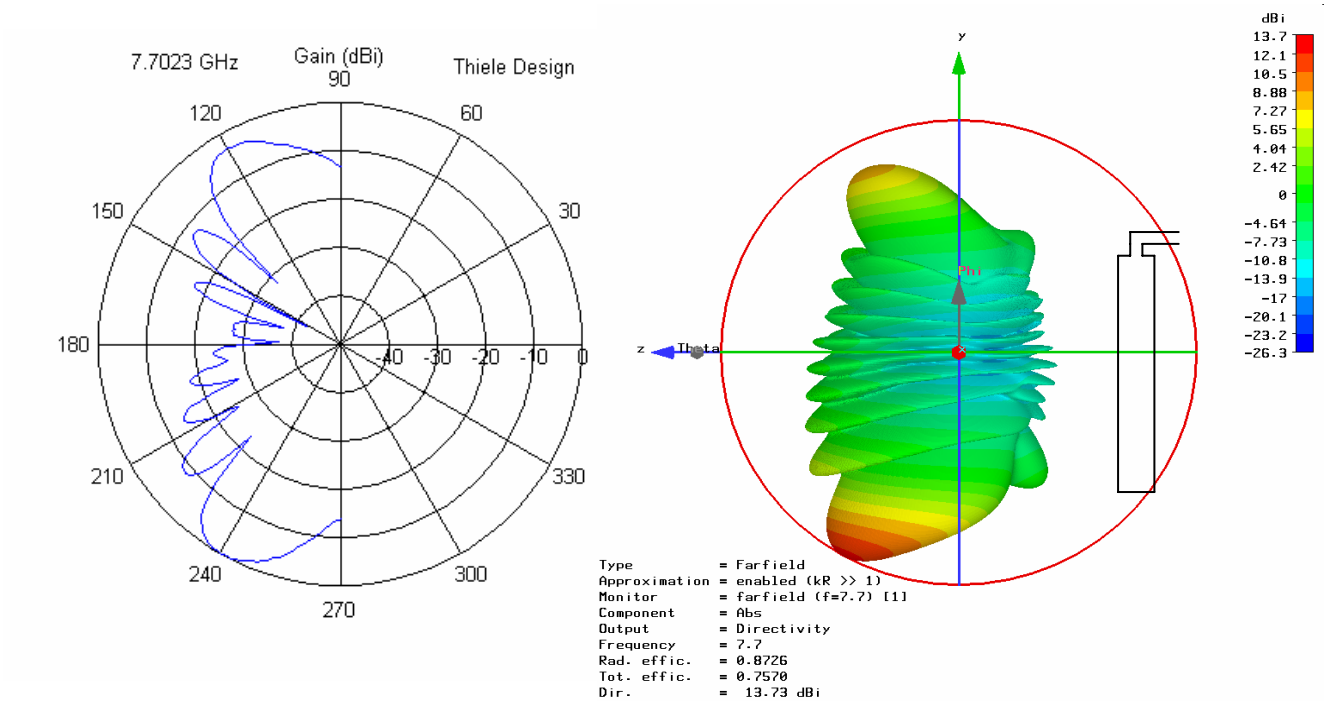

Figure 19: Measured (left) and Theoretical (right) comparison for 7.7 GHz.

A permanent CST microwave studio license has been purchased and we expect the new license to arrive any day. In the mean time, we have renewed multiple temporary licenses and Mr. John Reynolds and Mr. Michael Corwin have performed multiple simulations of different "half-width" configurations on a new computer purchased by RASCAL designated specifically for CEM simulations. RASCAL will continue to exhaust all methods of CEM modeling in efforts to aid in finding effective and applicable configurations of the leaky wave "half-width" technology.

Work Cited

1. W. Menzel, "A New Traveling-Wave Antenna in Microstrip", *Archiv fur Elektronik und Ubertragungstechnik (AEU)*, Band 33, Heft 4:137-140, April 1979.

2. J.S. Radcliffe, G.A. Thiele, and G. Zelinski, "A microstrip leaky wave antenna and its properties, *26th Antenna Measurement Tech. Assoc. Meeting*, St. Mountain, GA, Oct. 2004.

3. G.M. Zelinski, M.L. Hastriter, M.J. Havrilla, J.S. Radcliffe, A.J. Terzuoli, and G.A. Thiele, "FDTD analysis of a new leaky traveling wave antenna," submitted to the *2005 IEEE/ACES Intl. Conf.*, Honolulu, Hawaii, Apr. 2005.

4. L. Kempel, S.W. Schneider, J.S. Radcliffe, D.S. Janning, and G.A. Thiele, "FE-BI Analysis of a Leaky Wave Antenna with Resistive Sheet Termination," *2005 IEEE/ACES (Applied Computational Electromagnetics Society) Conference*, Honolulu, Hawaii, Apr. 2005. ***Presenter

5. L. Kempel, J.S. Radcliffe, S.W. Schneider, G.A. Thiele, "Comparison of Two Termination Schemes for a Half-width Leaky Wave Antenna," *2005 IEEE APS/URSI (Antennas & Propagation Society / Union of Radio Scientists International) Conference*, Washington DC, July 2005.

6. D. Killips, J.S. Radcliffe, L. Kempel, and S.W. Schneider, "Radiation by a Linear Array of Half-Width Leaky Wave Antennas," *2006 IEEE/ACES (Applied Computational Electromagnetics Society) Conference*, Miami, Florida, March 2006.

7. J.S. Radcliffe, G. Thiele, R. Penno, S.W. Schneider, and L. Kempel, "Microstrip Leaky Wave Antenna Performance on a Curved Surface," *2006 IEEE APS/URSI (Antennas & Propagation Society / Union of Radio Scientists International) Conference*, Albuquerque, NM, July 2006.

Radar Direction Finding Technique Using Four-arm Spiral Antennas

Purpose and Payoff

Direction Finding (DF) systems have long been an area of intense research in the RF division of the Sensors Directorate. DF system enhancement is imperative in order to improve upon the accuracy and effectiveness of Angle of Arrival (AoA) determination. There are presently two types of existing DF systems: wide band multi-mode and interferometers. Wide band multi-mode DF systems allow for a large bandwidth but present a low resolution because of high variance. Interferometers provide high accuracy through low variance but are narrow band and require a large number of s-element antennas (figure 1).

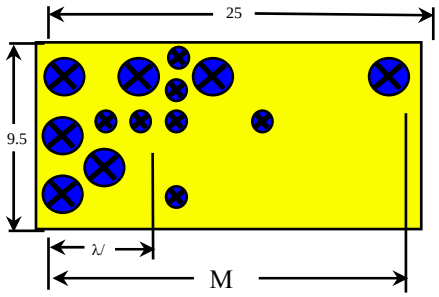

Figure 1: Interferometer DF system setup.

An effort has commenced in AFRL/SNRR's Radiation and Scattering Compact Antenna Laboratory (RASCAL) to incorporate a broadband DF system with high resolution using two multi-mode spiral antennas. This system will use Multi Signal Characterization (MUSIC) instead of phase comparison to obtain lower variance of estimates. Using a interferometer of multi-mode elements, we can provide high resolution without using numerous antennas (figure 2). The concept for this project was envisioned by Dr. Krish

Pasala from the University of Dayton while the RASCAL laboratory provides a suitable setting for the realization of this project.

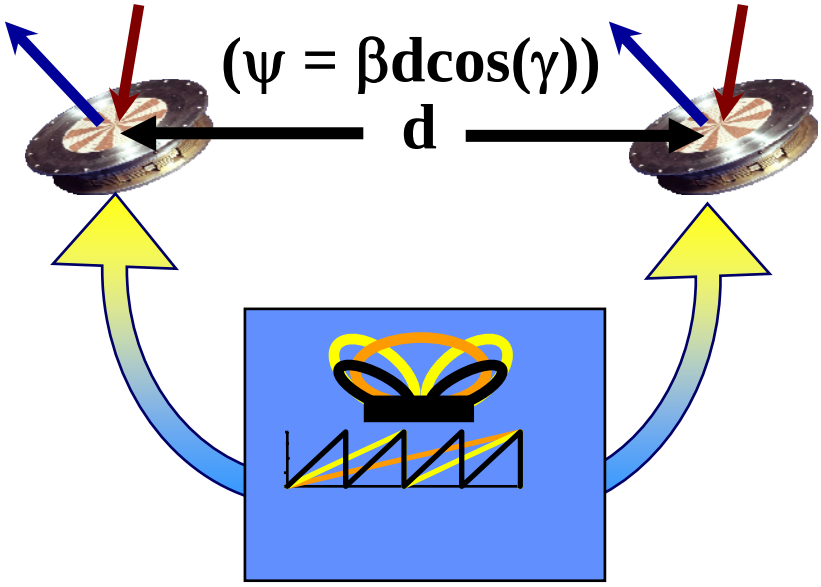

Figure 2: MUSIC DF system setup.

The proposed effort seeks to validate the performance of the MUSIC broadband DF system by assembling each subsystem, integrating all subsystems, and ascertain all effects of the system as determined by accurate measurements in RASCAL.

4-Arm Spiral Antenna Research

Much initial research went into understanding the traditional 4-arm spiral antenna. Studied specifically were phase progression, current distribution, spiral parameter calculations, mode analysis (figure 3) and mode forming. All research into each of these parameters will aid in the understanding, construction, and validation of the MUSIC direction finding system.

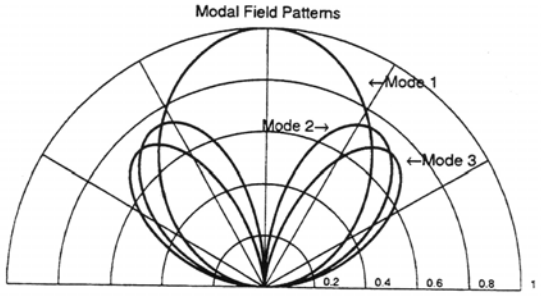

Fig. 3. Model magnitudes versus elevation.

Spiral Measurements

Numerous measurements were performed in AFRL/SNRR's RASCAL compact range. These measurements are being used to compare parameters of both 4-arm spiral antennas for performance precision of the MUSIC DF system.

In order to obtain accurate data from each spiral antenna, a phase-stationary test body was used in all 4-arm spiral measurements. When considering a (conformal) antenna in the presence of a conducting surface, once must make a careful evaluation of the performance of that antenna in an appropriate environment. An antenna test body is required to close the distance between a (conformal) antenna host surface and the designer's infinite ground plane model. The "almond" shaped test body owned by RASCAL and used for all 4-arm spiral measurements in this project is a documented, proven, and patented device for high performance antenna measurements. This "almond" test body incorporates a unique positioning system which provides a phase-stationary antenna aperture center under rotation of both azimuth and elevation. The result is that all 4-arm spiral measurements can be performed with the center of the spiral in a fixed position in the antenna test range incorporated in a test body of high performance with ground plane characteristics.

Conic azimuth cuts were taken at an elevation of $\theta = 20^{o}$ for all usable modes, both 4-arm spiral antennas, and both vertical and horizontal polarizations. Figure 4 shows data from these measurements from one mode and one frequency.

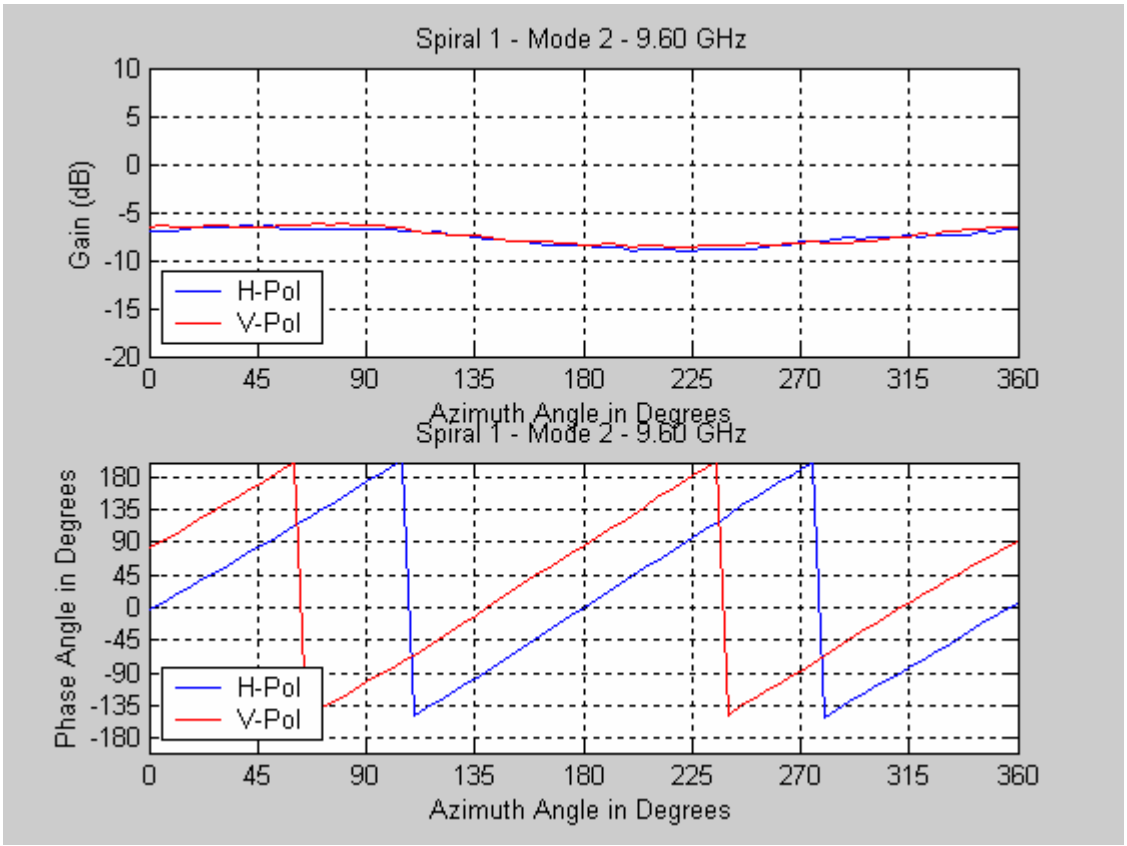

Figure 4: Azimuth measurement for Sprial 1, mode 2 at 9.6 GHz.

Obtaining phase data as a function of azimuth is arguably the most important data to be collected for the validation of accurate AoA determination. This 360° azimuth data reveals much information about the direction of the incoming signal(s). An example of results obtained can be seen in figure 4.

The phase-stationary test body is set up at a specific elevation angle from the center of the parabolic reflector (boresight). As noted in figure 5, the spiral antenna is then rotated 360° around the axis of symmetry as magnitude and phase data are collected at 5° azimuth increments. This process is repeated for modes 1, 2, and 3 for both 4-arm spiral antennas and was used to collect data at elevation angles of THETA = 20°, 40°, and 45°. Elevation angles of THETA = 40° and 45° are near the main beam peaks for modes 2 and 3, respectively. We determined the peaks of these modal main beams by performing elevation cuts.

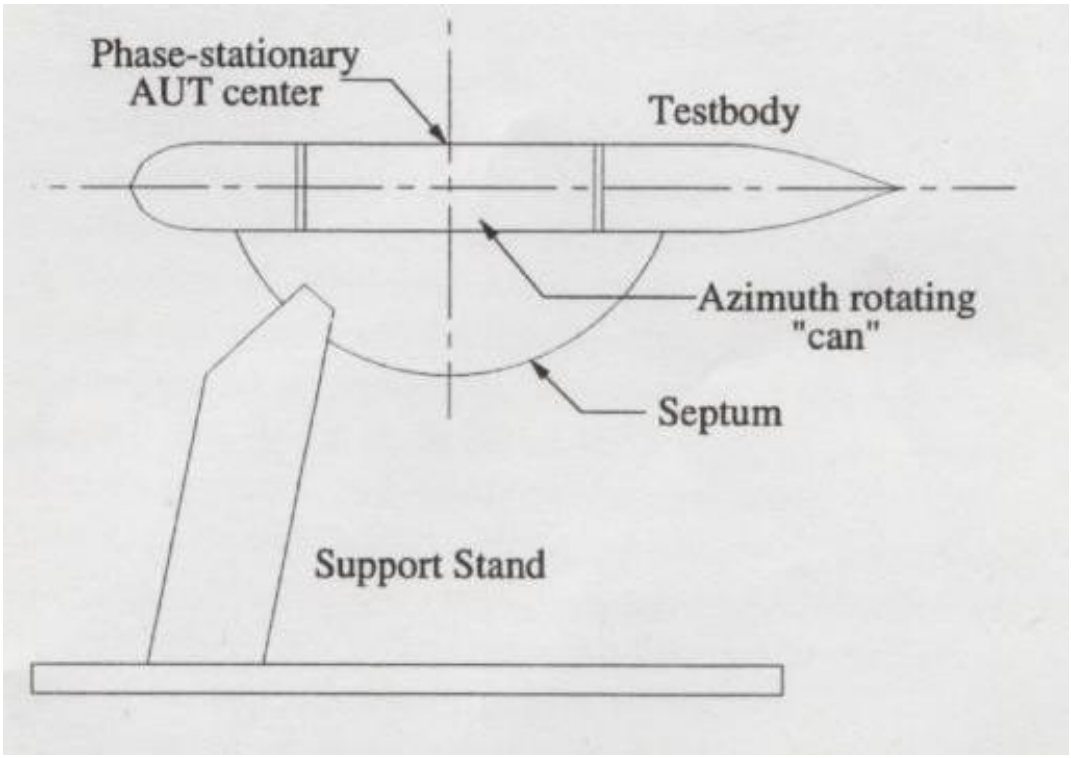

Figure 5: Phase stationary test body setup.

Elevation magnitude data provided the information of main beam peaks for modes 2 and 3. We found that as frequency increased, the mode 2 and 3 beams approached endfire; obviously, the values for main beam peaks did not consistently stay peaks atop the main beams as frequency increased.

The phase-stationary test body begins positioned at THETA = 90° elevation. The test body then rotates via the septum (see figure 5) a full 90° and terminates when the spiral is boresight to the parabolic reflector. The spiral is then itself rotated 180°, via the

can (see figure 5), and the elevation position reset to THETA = 90°. The original scan sequence is then repeated: The test body rotates via the septum another full 90° and terminates when the spiral is boresight to the parabolic reflector. This full process was then repeated for modes 1, 2, and 3 for both 4-arm spiral antennas; the magnitude data obtained was joined for each respective mode and full 180° elevation slices were obtained for an azimuth angle of PHI =0°. Figure 6 shows an example of elevation results obtained.

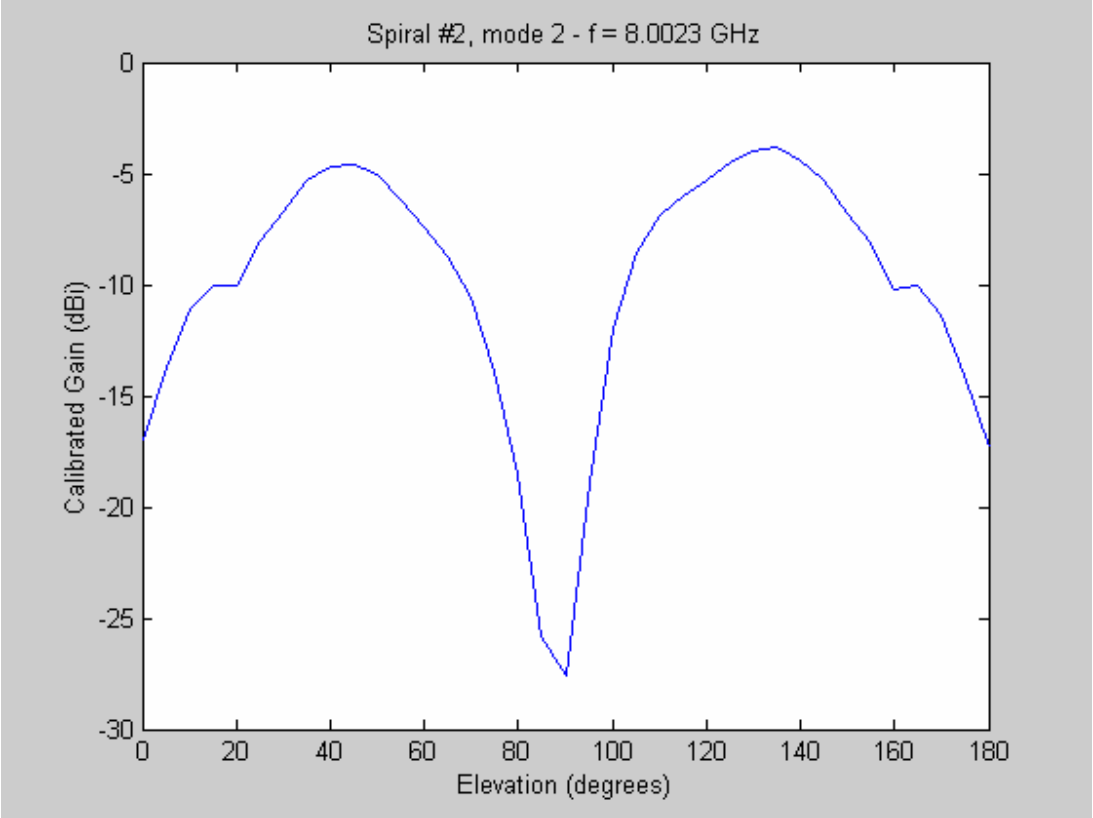

Figure 6: Elevation measurement for spiral #2, mode 2, at 5.5GHz.

MUSIC Algorithm Simulation

A simulation of the MUSIC algorithm was created using MATLAB. This simulation asked for signal and array parameters and given these parameters, used the MUSIC algorithm to determine AoA and estimate the spectrum. Parameters given are signal amplitude, signal frequencies, the number of data points taken, the number of elements in the linear array, the wavelengths between each element in the array, the AoA of two or more incoming signals, and the signal-to-noise ratio (SNR) of the signals. Using these given signals, the MUSIC algorithm uses signal processing techniques to estimate the spectrum and AoA of the signals. Figure 8 shows three results of this MUSIC simulation technique. The first result shows two signals arriving 15^{o} apart, the second result shows two signals arriving 10^{o} apart, and the last result shows two signals 5^{o} apart, respectively left to right.

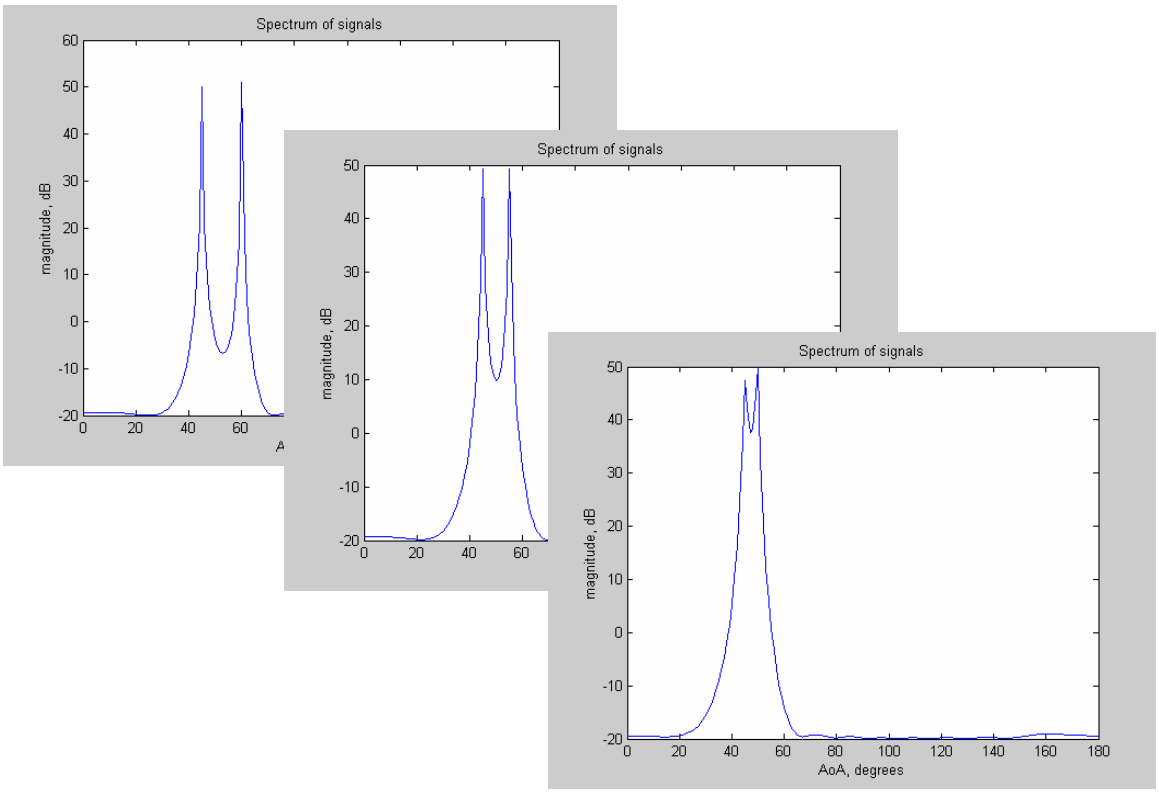

Figure 8: MUSIC algorithm simulation using MATLAB for two distinct signals at close incident angles.

Through these simulation results, it is easy to see the high resolution that MUSIC enables along with the low variance of estimates. These factors are what allow the MUSIC algorithm to be so appealing for a modern DF system.

Work Cited

1. Pasala, Krishna, and Penno, R., "Theory of Angle Estimation Using a Multiarm Spiral Antenna," *IEEE Transactions on Aerospace and Electronic Systems*, **37**, 1 (January 2001), 123-133.

2. Pasala, Krishna, Penno, R., and Schneider, S., "Novel Wideband Multi-mode Hybrid Interferometer System," *IEEE Transactions on Aerospace and Electronic Systems*, **37**, 4 (October 2003), 1396-1406.

3. J.S. Radcliffe, K. Pasala, and S.W. Schneider, "The Calibration of Four-arm Spiral Modal Measurements for Angle-of-Arrival Determination," *27th Antenna Measurement Techniques Association Annual Symposium Proceedings*, Newport, RI, November 2005. ***Presenter

4. J.S. Radcliffe, “Radar Direction Finding Technique Using Spiral Antennas,” *AFRL Horizons magazine*, April 2006, Volume 7, Number 2, pg. 13.